



Missouri University of Science and Technology
Scholars' Mine

Chemistry Faculty Research & Creative Works

Chemistry

14 Jan 2013

Surface Temperature Effects on the Dynamics of N₂ Eley-Rideal Recombination on W(100)

Ernesto Quintas-Sánchez

Missouri University of Science and Technology, quintassancheze@mst.edu

C. Crespos

P. Larrégaray

J. C. Rayez

et. al. For a complete list of authors, see https://scholarsmine.mst.edu/chem_facwork/3088

Follow this and additional works at: https://scholarsmine.mst.edu/chem_facwork

 Part of the [Chemistry Commons](#), and the [Physics Commons](#)

Recommended Citation

E. Quintas-Sánchez et al., "Surface Temperature Effects on the Dynamics of N₂ Eley-Rideal Recombination on W(100)," *Journal of Chemical Physics*, vol. 138, no. 2, American Institute of Physics (AIP) Publishing, Jan 2013.

The definitive version is available at <https://doi.org/10.1063/1.4774024>

This Article - Journal is brought to you for free and open access by Scholars' Mine. It has been accepted for inclusion in Chemistry Faculty Research & Creative Works by an authorized administrator of Scholars' Mine. This work is protected by U. S. Copyright Law. Unauthorized use including reproduction for redistribution requires the permission of the copyright holder. For more information, please contact scholarsmine@mst.edu.

Surface temperature effects on the dynamics of N₂ Eley-Rideal recombination on W(100)

E. Quintas-Sánchez,^{1,2} C. Crespos,^{2,a)} P. Larrégaray,² J-C. Rayez,² L. Martin-Gondre,³ and J. Rubayo-Soneira¹

¹*InSTEC, Ave. Salvador Allende esq. Luaces, 10600 La Habana, Cuba*

²*University Bordeaux, ISM, UMR5255, F-33400 Talence, France*

³*Centro de Física de Materiales CFM/MPC (CSIS-UPV/EHU), P. Manuel de Lardizabal 4, 20018 San Sebastian, Spain*

(Received 11 October 2012; accepted 18 December 2012; published online 14 January 2013)

Quasiclassical trajectories simulations are performed to study the influence of surface temperature on the dynamics of a N atom colliding a N-preadsorbed W(100) surface under normal incidence. A generalized Langevin surface oscillator scheme is used to allow energy transfer between the nitrogen atoms and the surface. The influence of the surface temperature on the N₂ formed molecules via Eley-Rideal recombination is analyzed at T = 300, 800, and 1500 K. Ro-vibrational distributions of the N₂ molecules are only slightly affected by the presence of the thermal bath whereas kinetic energy is rather strongly decreased when going from a static surface model to a moving surface one. In terms of reactivity, the moving surface model leads to an increase of atomic trapping cross section yielding to an increase of the so-called hot atoms population and a decrease of the direct Eley-Rideal cross section. The energy exchange between the surface and the nitrogen atoms is semi-quantitatively interpreted by a simple binary collision model. © 2013 American Institute of Physics. [<http://dx.doi.org/10.1063/1.4774024>]

I. INTRODUCTION

The reactivity at the gas-solid interface plays a key role in various domains of application, as for example the heterogeneous catalysis,^{1–3} the chemistry of the atmospheric⁴ and interstellar media,^{5–7} the behavior of materials exposed to plasmas,^{8–13} or the surface functionalization by self-assembled monolayers growth.^{14–17} From a more fundamental point of view, studying chemical processes at surfaces has known a growing interest within the last twenty years with the progress of surface science experimental techniques^{18,19} and theoretical simulations.^{20–24} The dynamics of hydrogen molecular recombination on metal surfaces has been extensively studied both experimentally^{25–27} and theoretically,^{28–40} revealing a rather complex variety of mechanisms. Among these elementary gas-surface processes, the molecular recombination following an Eley-Rideal (ER) mechanism, where an incoming atom from the gas phase reacts with an atom previously adsorbed on a surface, is known to produce highly rovibrational excited molecules.^{25–27} The ER mechanism is often seen as a single collision process, but the recombinative event can occur through a multiple collision process; the latter is usually defined as hot-atom (HA) mechanism.^{31,35,41–46} The HA reaction also leads to hot products since the impinging atom keeps a large part of its kinetic initial energy even after many rebounds in the vicinity of the surface. The atom does not thermalize at the temperature of the surface within a *ps* timescale. Previous works, mostly focused on H₂ formation over several metal surfaces, have shown that the HA cross section is much larger (typically one order of

magnitude) than the ER one.^{29,31,32,35} As a consequence, molecular recombination on surfaces results primarily from HA reactive pathways leading to large cross sections and a strong dependence of the preadsorbed atoms coverage. H₂ formation via ER or HA mechanisms usually exhibits large exothermicity and the absence of potential energy barriers along reaction path, which justifies the production of hot molecules. Recently, we have studied the N₂ ER recombination dynamics on W(100).^{47–49} The peculiarity of this system, beyond the fact that N₂ is a benchmark molecule in the framework of heavy diatomic molecules reacting on surfaces,^{50–67} is the presence of a potential energy bump of about 500 meV in the entrance channel located above the adsorbate.⁴⁹ The N-N interaction is thus repulsive in the medium range (2.5–3.5 Å) upon approach of the gas phase atom towards the preadsorbed one for impact parameters lower than 1.0 Å (the impact parameter is defined as the projection of the N-N distance on the surface plane). Despite the existence of the entrance channel energy bump, non-activated pathways exist for ER reaction. Nevertheless, the cross section for direct one-collision ER reaction presents an unusual threshold of 0.53 eV due to dynamical effects governed by an interplay between N-N repulsion and strong N-surface attraction. At energies below the threshold, the impinging atoms are deflected by the repulsive potential bump, and are unable to find the non-activated ways leading to a majority of trapped HA production together with a high proportion of reflected back atoms. At higher energies, the potential energy bump effect vanishes and gas phase atoms grab the preadsorbed ones in one rebound on the surface atoms. In the present work, we analyze the dynamics of these direct recombinative events, and more specifically the

^{a)} Author to whom correspondence should be addressed.

features of the formed molecules, as a function of the surface temperature within a moving surface model allowing energy exchange between the N atoms and the surface.

The paper is organized as follows. In Sec. II, we give some details on the calculations and the methodology employed. In Sec. III, we present and discuss the results of the dynamics study. Finally, we summarize and conclude in Sec. IV.

II. METHODOLOGY

As detailed in our previous papers,^{47–49} the ER recombination of nitrogen on W(100) has been studied theoretically by performing quasi-classical trajectories (QCT) simulations. Trajectories are numerically integrated on a single potential energy surface (PES), which corresponds to the ground adiabatic electronic state. The chosen PES is suitable for the reaction of an impinging nitrogen atom (projectile) reacting with a single preadsorbed nitrogen atom (target) on the W(100) surface. A Flexible Periodic London-Eyring-Polanyi-Sato (FPLEPS) model^{55–57} has been used to account for all the features of the interaction potential revealed by the electronic structure calculations.^{64,65} Density functional theory (DFT)^{68–77} calculations have shown the existence of a potential repulsive bump located in the ER entrance channel, for a projectile/target distance of about 2.5 to 3.6 Å, which is a quite unusual feature in the context of ER reaction studies.⁴⁹ The ER nitrogen recombination mechanism is studied within the approximation of a moving surface model by incorporating a 3-dimensional surface oscillator connected to a so-called ghost atom, itself connected to a thermal bath (Generalized Langevin Oscillator (GLO) model).^{78–83} This moving surface model accounts for energy exchange with the surface. In our simulations, one has chosen to work with the unreconstructed W(100) surface. This choice imposes to analyze the surface temperature effect at temperature higher than 200 K since the W(100) is known to undergo a structural phase transition below this temperature leading to a $c(2 \times 2)$ zigzag surface atoms rearrangement.^{84,85} Electronic effects such as electron/hole pair excitations are not included in our simulations. Such non-adiabatic effects have been shown to negligibly influence the N₂ dissociative adsorption on W and one suggests that it will be negligible too in ER short-time processes.^{86–90}

The initial conditions of our classical trajectories are identical to the ones used for the static surface model in previous work.⁴⁹ The only difference resides in the sampling of the surface oscillator initial position and speed, which follows a Boltzmann distribution. As a matter of fact: (i) the target atom is adsorbed on the fourfold hollow site (which has been shown to be the lowest energy adsorption site^{64,65}) and its initial energy is equal to the zero point energy (ZPE) of 56 meV shared between the three vibrational modes, (ii) the projectile atom, coming from an altitude of 8.0 Å located in the asymptotic region, approaches the surface at normal incidence, (iii) the initial position of the projectile above the surface is uniformly sampled within the surface unit cell (actually, due to symmetry considerations only an octant of the unit cell has to be sampled), and (iv) as already said, the surface oscillator, together with the ghost atom positions and speeds, belongs to a

canonical ensemble following a Boltzmann law. In our previous study, all the possible exit channels have been defined in details.⁴⁹ The ER reaction is supposed to take place whenever the altitude of both N atoms get greater than the initial altitude of the projectile with a N₂ molecular center of mass momentum directed towards vacuum. One additional requirement is the fact that the N₂ momentum has changed its sign only once all along the trajectory, insuring that molecules are formed in only one rebound of the N-N center of mass. Such trajectories are close to what is defined as a real direct ER mechanism. Trajectories are integrated up to the projectile's first rebound, then, the N-N distance is checked at each time step. If this distance gets larger than the maximum value ascribable to the N₂ diatomic molecule, r_{NN} , the dynamical event is classified as HA formation. r_{NN} is chosen large enough for the N-N interaction to be negligible with respect to the N-W(100) one. As a consequence, the total interaction energy reduces to the sum of two separated atom-surface interactions. In practice, the results presented below are insensitive to the value of r_{NN} for $r_{NN} \geq 2.5$ Å in the case of the static surface. Two HA channels are considered depending on the final energy of both N atoms. In the *metastable* HA process (mHA), the total energy of either nitrogen atom is greater than the minimum energy to escape from surface attraction whereas in the *bound* HA channel (bHA) both N atoms are trapped close to the surface. mHA trajectories are further integrated and classified as direct reflections if they do not involve any additional rebound. Furthermore, it is important to mention that our model cannot properly simulate the HA mechanism, which has been shown to be rather complex and strongly dependent of the surface coverage.²⁹ In the present study, we work at zero surface coverage limit.

In order to focus on the influence of the surface temperature on the reactivity, one has chosen to select two different values of the initial translational energy of the projectile (defined in the following as projectile collision energy, E_p), which are representatives of the medium collision energy range with $E_p = 1.0$ eV and the large energy range with $E_p = 2.6$ eV, when considering the ER cross section as a function of E_p .⁴⁹ The ER cross section together with the bHA, and the mHA formation cross sections as a function of E_p are plotted on Fig. 1. These results have been obtained for a static surface model (see previous work for more details⁴⁹).

III. RESULTS AND DISCUSSION

A. Results for the moving surface model: Surface temperature effect

The influence of surface motion on the ER reactivity is analyzed at various surface temperatures ($T = 300, 800,$ and 1500 K) for two values of the initial kinetic energy of the projectile atom ($E_p = 1.0$ and 2.6 eV). For interpretation purposes, QCT simulations are also performed for two limit cases: (i) the static surface case and (ii) the moving surface case at $T = 0$ K. The $T = 0$ K limit has no physical meaning since, as already discussed, the unreconstructed W(100) exists only for temperature above 200 K. As a consequence, it is important to note that simulations on both static surface and

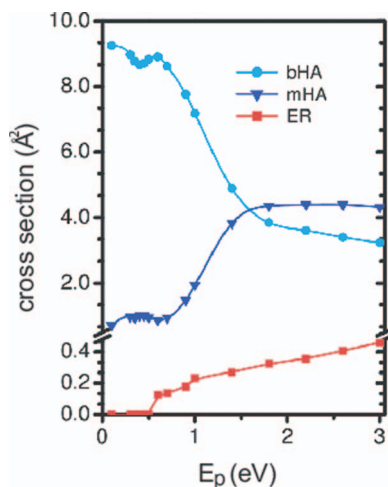


FIG. 1. Cross sections (in \AA^2) for *bound* (bHA, circles), *metastable* (mHA, triangles) HA formation, and ER reaction (squares) obtained within a static surface model.

$T = 0$ K moving surface are only carried out to provide elements for a better understanding of the dynamics features at $T = 300, 800,$ and 1500 K. The results of QCT simulations are reported in Table I where all the exit channels cross sections are represented.

The HA formation pathways dominate in all cases. At the first step, when allowing the surface to move, the bHA cross section increases. Then, this cross section slowly decreases with temperature increase from $T = 300$ to 1500 K but still remains higher than the static surface cross section. Everything happens as if the projectile energy exchange with the surface was in favor of a longer residence time of the impinging atom at the vicinity of the surface. The conjugation of an attractive potential together with a significant energy transfer to the surface leads to a trapping of the projectile close to the surface. For the same reason, the mHA cross section decreases when energy transfer to the surface is allowed. An important part of the mHA of the static model case converts to bHA for the moving surface. As expected, the atomic reflection cross section (P_{REF}) decreases with the inclusion of surface motion. Focusing on ER reaction cross section (P_{ER}), energy exchange

TABLE I. Exit channels cross sections (in \AA^2) for static and moving surface models ($T = 0, 300, 800, 1500$ K) at two collision energies $E_p = 1.0$ and 2.6 eV.

$E_p = 1.0$ eV	P_{ER}	P_{REF}	P_{bHA}	P_{mHA}
Static-surface	0.23	0.64	7.18	1.94
0 K	0.12	0.24	9.20	0.43
300 K	0.13	0.24	9.18	0.45
800 K	0.14	0.25	9.06	0.52
1500 K	0.16	0.25	8.89	0.67
$E_p = 2.6$ eV				
Static-surface	0.41	1.40	3.39	4.39
0 K	0.26	0.74	6.31	2.50
300 K	0.25	0.72	6.25	2.57
800 K	0.27	0.69	6.15	2.64
1500 K	0.30	0.66	6.10	2.67

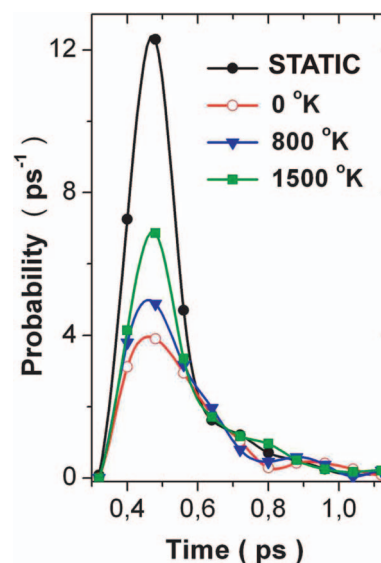


FIG. 2. Distribution of ER trajectories simulation time as a function of temperature. The initial kinetic energy of the incident atoms is 1.0 eV.

with the surface clearly cancels some ER reactive events and the cross section first drops down (from static surface to $T = 0$ K) and subsequently increases (from $T = 0$ K to higher temperatures). Still, when the surface motion is taken into account, the ER reaction cross section remains small, whatever the temperature of surface atoms being always below 0.16\AA^2 for $E_p = 1.0$ eV (and below 0.30\AA^2 for $E_p = 2.6$ eV).

In the following, the discussion specifically focuses on ER reaction dynamics and how the surface temperature influences the ER reactivity. In Fig. 2, distributions of ER trajectories simulation times (defined as the total time from the departure of the trajectory to the time at which a formed N_2 molecule is 8.0\AA above the surface) are plotted for three different temperatures ($T = 0, 800, 1500$ K) and for the static surface case. Curves are normalized such that the area under each of them is equal to the cross section of ER recombination as listed in Table I. The direct ER recombination takes place in a *sub-ps* time scale, leading to a typical interaction time between the two N atoms and the surface lower than 100 fs. The majority of the ER trajectories have already escaped from the surface 0.5 ps after having started, this time being very close to the mean direct reflection time for projectile atoms colliding a surface clean of pre-adsorbed atoms ($t = 0.4$ ps at $E_p = 1.0$ eV). As shown in Fig. 2, the influence of the surface motion on the ER reaction times is rather significant when going from a static surface model to a moving surface one. The proportion of shortest simulation times decreases whereas longer times remain almost constant, as if the inclusion of energy transfer with the surface canceled the ER short time reactions. When increasing temperature, the relative importance of the fast reactive trajectories increases. The ER exit channel involves only one rebound of the two atoms center of mass. Thus, the fast and slower ER reactions exhibit roughly the same mechanism. The difference in reaction time is thus due to: (i) a difference in the exit angles of the formed molecules, (ii) a difference in the center of mass exit kinetic energy.

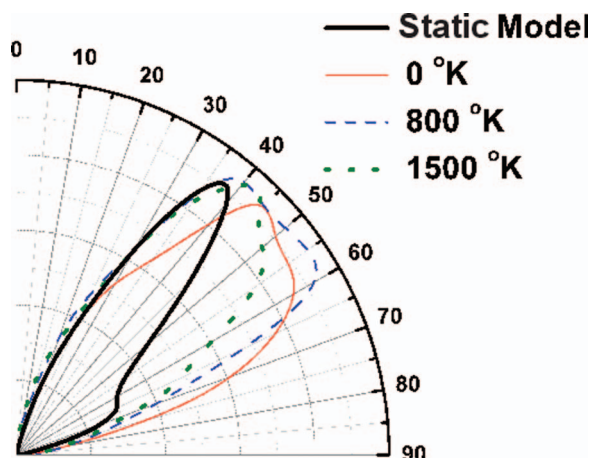


FIG. 3. Polar plot of the angular distribution of N_2 formed molecules for different surface temperatures and a collision energy of the projectile atom: $E_p = 1.0$ eV. Each distribution is normalized to unity.

Fig. 3 depicts the exit angle distributions of the formed N_2 molecules for the three different temperatures $T = 0, 800, 1500$ K, as indicated. Each distribution is normalized to unity. The angular distributions of the formed molecules are spread out between 30 and 70 degrees. A shift of the distributions to smallest values of the exit angle when going from $T = 0$ to 800 and 1500 K is observed. The static surface model angular distribution is also plotted for comparison. The increase of temperature slowly modifies the distributions in direction of the static surface case for which the exit angles are rather concentrated around the low value of 38 degrees.

To understand further the influence of temperature on the ER reactivity, it is important to analyze the energetics of the reaction. The $N_2/W(100)$ ER recombination reaction is strongly exothermic. So that the formed molecules might be characterized by high internal energy excitation. Considering the PES used for the QCT simulations the adsorption energy for a N atom in a W(100) surface is -7.36 eV and the bounding energy of a N_2 molecule in vacuum is -9.9 eV. Thus, the exothermicity of the N_2 recombination on W(100) is 2.54 eV. As a consequence, the maximum available molecular energy E_T^{MAX} (considering a static surface model) for the formed molecule is 2.54 eV plus the zero point energy of the adsorbed atom (≈ 0.06 eV), plus the initial collision energy of the projectile E_p ($E_T^{MAX} = 3.6$ eV for $E_p = 1.0$ eV and $E_T^{MAX} = 5.2$ eV for $E_p = 2.6$ eV). During an ER event, only one part of E_T^{MAX} is transferred into the translational, and ro-vibrational degrees of freedom of the N_2 molecule and the remaining part into the surface. This energy partitioning mechanism is an important aspect of the atoms recombination at surfaces.

In Fig. 4, we plot the probability distributions for the total final molecular energy E_T of the recombined molecules, $P(E_T)$, for different surface temperatures. The curves are normalized to the reaction cross sections of Table I. Most of the maximum available energy (referred in the figures as static Model straight line) is transferred to the molecule. At $T = 0$ K, the distribution is sharply peaked around 2.7 eV (75% of the maximum available energy) for $E_p = 1.0$ eV and 4.0 eV (77% of the maximum available en-

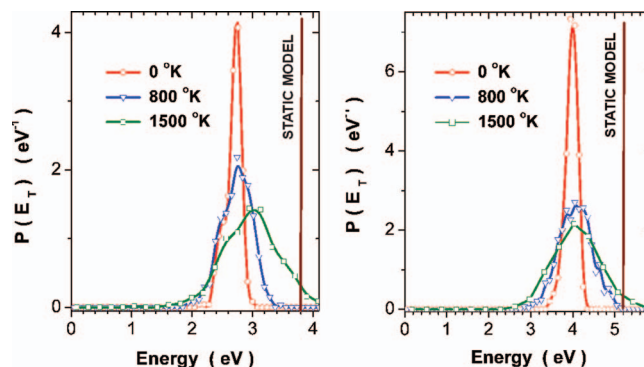


FIG. 4. Distributions of the total final energy, E_T , (rotation + vibration + translation) of the N_2 molecules for different collision energies of the projectile atom: $E_p = 1.0$ eV (left) and $E_p = 2.6$ eV (right) and for $T = 0, 800, 1500$ K. The maximum available final energy, E_T^{MAX} , is indicated for each plot by a vertical line, which corresponds to the static surface model case. Lines are drawn to guide the eye.

ergy) for $E_p = 2.6$ eV. For higher temperature, and whatever the initial kinetic energy of the projectile, the distributions are shifted towards higher values of energy (from $T = 0$ K to $T = 1500$ K the shift is roughly 0.3 eV for $E_p = 1.0$ eV and 0.1 eV for $E_p = 2.6$ eV) and get wider. At $T = 1500$ K, part of the molecules are produced with higher total energy than that predicted by the static surface model, implying energy has been transferred from the surface to the molecule.

The mean energy value transferred to the surface $\langle \Delta E \rangle = \langle E_T^{MAX} - E_T \rangle$, the mean kinetic energy of the center of mass $\langle K_{CM} \rangle$ and the mean ro-vibrational energy $\langle E_{VR} \rangle$ of the formed molecules are reported in Table II for $T = 0, 300, 800$, and 1500 K at $E_p = 1.0$ and 2.6 eV. The static surface case is also presented. The mean energy dissipated to the surface decreases with surface temperature, and increases with kinetic energy of the incident atom. As the energy of the projectile increases the amount of energy dissipated to the substrate become less sensitive to the surface temperature. The decrease observed in $\langle \Delta E \rangle$ with the temperature (0.3 eV for $E_p = 1.0$ eV and 0.14 eV for $E_p = 2.6$ eV), is in agreement with the shift noticed in the total energy of the product N_2 molecules when the temperature increases (see Fig. 4).

The mean kinetic energy of the molecules, $\langle K_{CM} \rangle$, drops significantly when the surface is allowed to move and tends to increase with the surface temperature. When the surface temperature increases the projectile atom seems to release less energy to the surface. The formed molecule escapes the surface with a higher translational energy and a smallest exit

TABLE II. Energetics of direct ER reactions as a function of temperature. All energies of the table are given in eV.

Temp. (°K)	1 eV			2.6 eV		
	$\langle \Delta E \rangle$	$\langle K_{CM} \rangle$	$\langle E_{VR} \rangle$	$\langle \Delta E \rangle$	$\langle K_{CM} \rangle$	$\langle E_{VR} \rangle$
Static-surface	...	2.39	1.2	...	3.11	2.07
0	0.91	1.39	1.29	1.23	1.78	2.18
300	0.86	1.56	1.17	1.20	1.81	2.18
800	0.81	1.60	1.18	1.13	1.99	2.07
1500	0.61	1.76	1.22	1.09	2.05	2.05

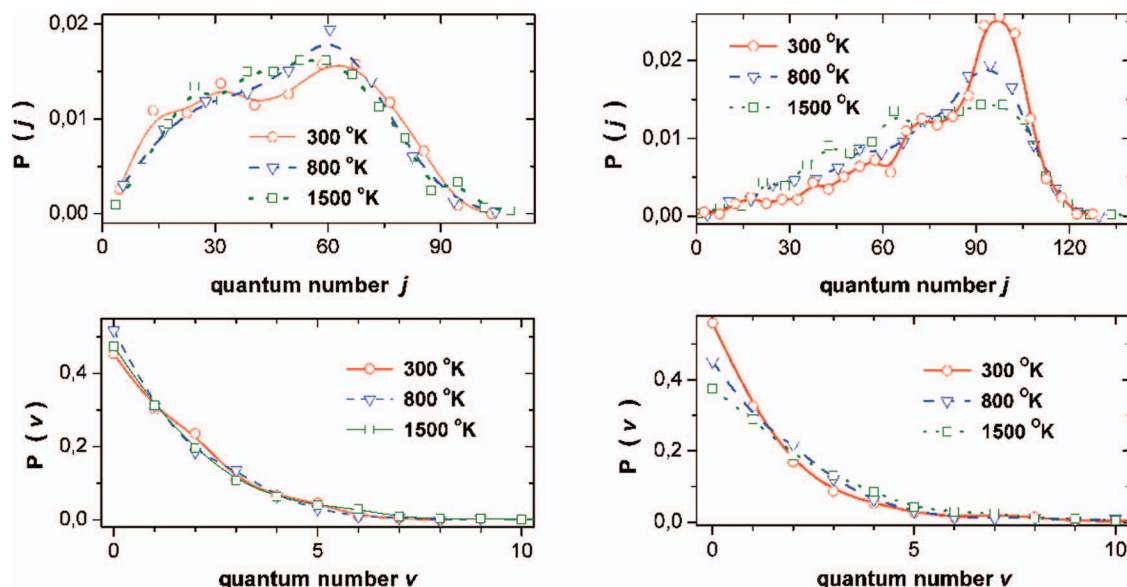


FIG. 5. Rotational (up) and vibrational (down) distributions of the formed N_2 molecules for different kinetic energies of the projectile atom: $E_p = 1.0$ eV (left) and $E_p = 2.6$ eV (right). Each distribution is normalized to 1. The results are shown for different surface temperatures, as indicated. Lines are drawn to guide the eye.

angle leading to shortest reaction times trajectories on average. The fraction of energy, imparted to N_2 translation, $f_{KE} = \langle K_{CM} \rangle / E_T$, is equal to 0.66 for $E_p = 1.0$ eV and 0.60 for $E_p = 2.6$ eV for the static surface, pointing out that the major part of the available energy goes to the kinetic energy of the formed molecules. When the surface atoms motion is taken into account, the partition between internal (vibrational plus rotational) and kinetic energy of the formed molecules is more balanced. For $E_p = 1.0$ eV, f_{KE} goes from 0.52 to 0.59, and for $E_p = 2.6$ eV, f_{KE} goes from 0.45 to 0.50 when the surface temperature increases from 0 K to 1500 K.

The decrease in the mean kinetic energy of the formed molecules, when the lattice motion is included in the simulations, corresponds approximately to the amount of energy dissipated to the substrate. Leading to the conclusion that the mean ro-vibrational energy should be almost independent of the temperature. The simulation results for $\langle E_{VR} \rangle$ confirm this point since the variation of $\langle E_{VR} \rangle$ with respect to the static case is at most 7.5% for $E_p = 1.0$ eV and 5.3% for $E_p = 2.6$ eV. In other terms, the variation of $\langle E_{VR} \rangle$ with temperature does not follow a monotonous behavior as it is the case for the other observables. Rotational and vibrational state distributions for different surface temperatures are in Fig. 5. Each distribution is normalized to unity. The effect of the temperature is only very minor for molecule ro-vibrational distributions. This is consistent with experimental observation in other systems that the internal energy of the molecules formed by direct recombination mechanisms does not change with the temperature of the surface, unlike Langmuir-Hinshelwood recombination reaction type.²⁶

By looking more closely at $E_p = 2.6$ eV, one can observe that rotation slightly cools down with temperature growth at the expense of the vibration, which is slightly enhanced. For $E_p = 1.0$ eV, there is no remarkable effect of the temperature.

As already evidenced by both experimental^{25,27,91} and quasi-classical static-surface studies^{43,44} of HD recombina-

tion over Cu(111) surface, the present simulations of N_2 molecules formation on W(100) surface exhibit products with high vibrational and rotational excited states. It has to be noticed that rather different behavior was observed on HD recombination studies on Ni(100),^{29,31,32} where relatively weak internal excitation of the product is reported.

B. Energy transfer interpretation using a simple collision model

As presented in a previous work,⁴⁹ most of the projectile atoms are first deflected by the potential bump (located above the target atom position) to regions where the PES is attractive leading to an acceleration of the projectile in direction of W surface atoms. After bouncing off a W atom, the projectile is redirected towards the target leading to the formation of the molecule. As a consequence, accounting for

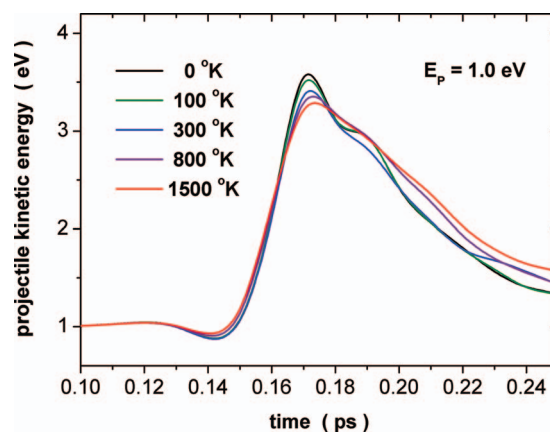


FIG. 6. Mean projectile kinetic energy as a function of trajectories integration time at various surface temperature for an initial kinetic energy of 1.0 eV.

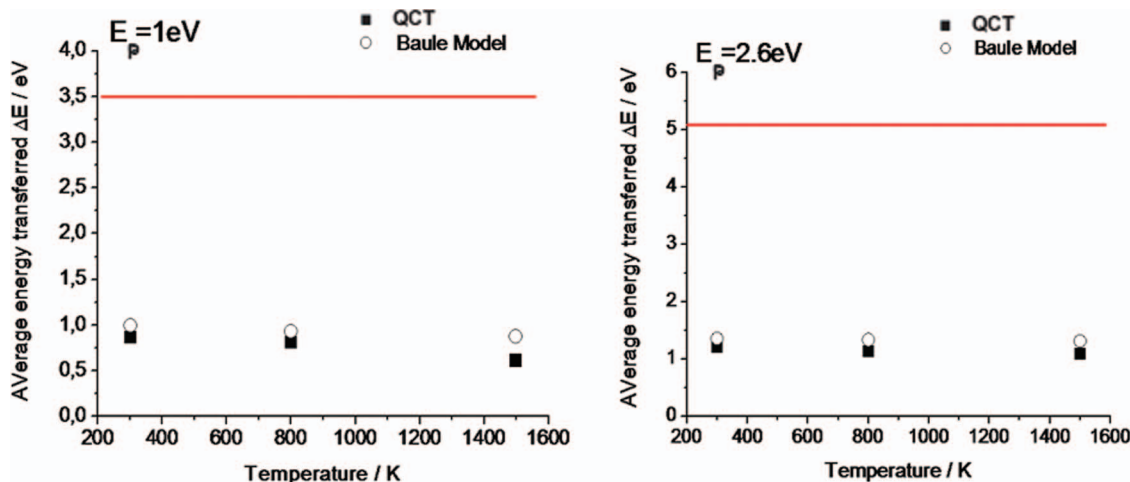


FIG. 7. Comparison between the projectile-surface energy transfer calculated using a simple collision modified Baule model (empty circles) and the results of the QCT simulations (plain square). Red lines indicate the maximum energy available for the formed molecule if no energy exchange with the surface is allowed.

projectile energy transfer to the surface is expected to modify ER dynamical observables. Fig. 6 shows the mean kinetic energy of the projectile atom (calculated by an average over the trajectories leading to ER recombinations) as a function of propagation time for the different surface temperatures under study and an initial kinetic energy of 1.0 eV. The strongly binding potential of N atom to W(100) causes the projectile to be accelerated by gaining approximately 2.5 eV of kinetic energy before bouncing off the surface at about $t = 0.17$ ps. After the collision, the atom is slowed down partially due to a significant transfer of energy to the surface. The interesting point is the fact that the amount of energy ΔE released in the surface can be evaluated by using a simple two body collision model, which differs to the original Baule model⁹² by the addition of a temperature dependent term proportional to $(k_B T)$.^{29,93}

$$\Delta E = \frac{4\mu}{(1 + \mu)^2} (E_{coll}^* - k_B T), \quad (1)$$

where ΔE is the energy transferred through a unique collision between a light body of mass m (in our case m will take the value of a nitrogen atom mass) and an heavier body of mass M (in our case M will be set equal to the mass of a W atom), μ being defined as the ratio $\mu = m/M$. E_{coll}^* represents the mean kinetic energy of the light mass m right before collision (the collision time has been chosen as the one corresponding to the maximum of the projectile kinetic energy curve, and the E_{coll}^* has been set up as the energy corresponding to this maximum depending on the surface temperature), determined by our trajectories simulations. Using the information taken from the classical trajectories (see Fig. 6), the value of E_{coll}^* can be determined for each surface temperature and the evaluation of the mean energy transfer ΔE predicted by the modified Baule model can be calculated. As can be seen on Fig. 7, the comparison between the energy transfer calculated from a simple collision model and the results extracted from the ER trajectories is amazingly good. Everything happens as if the energy transfer between the projectile atom and the surface was fully represented by a unique collision between the im-

pinging N atom and a W atom of the surface. The temperature dependent term does not play a major role since it is at most equal to 34 meV when $T = 1500$ K. As a consequence, the variation of the energy transfer with the surface temperature seems to be only due to the fact that for $T = 0$ K the projectile atoms are on average more accelerated than for $T = 1500$ K. This result is rather puzzling since the influence of the

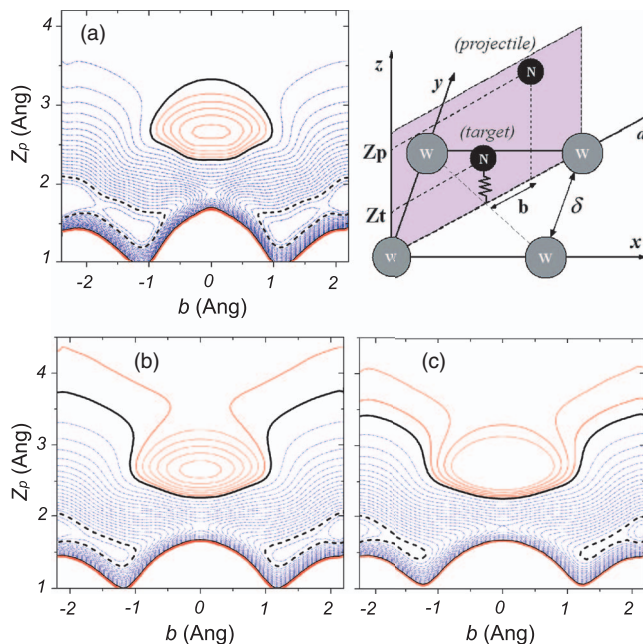


FIG. 8. (a) Potential energy (Z_p, b) 2D-cut along the diagonal plane highlighted on the upper right panel where the coordinate system and W(100) unitary cell are presented. The Cartesian reference frame is originated on a Tungsten top surface atom (grey circles). Black circles represent nitrogen atoms. Z_p and Z_t stand, respectively, for the altitude of the projectile and the target atom. The parameter b is defined as the impact parameter. $\delta = 3.175$ Å. Boltzmann thermal averaged (Z_p, b) 2D-cut potentials for $T = 800$ K (b) and 1500 K (c). Black lines correspond to zero energy isovalues (projectile atom at the infinite of the surface), red lines are positive values of the potentials, and blue dotted lines are negative values. The bold dotted lines encircle the most attractive regions of the potentials.

surface atoms motion on the projectile attraction is not straightforward.

In order to understand the temperature effect on the mean projectile kinetic energy, Boltzmann thermal averaged potentials 2D-cuts has been drawn for $T = 800$ and 1500 K in Fig. 8 (for comparison purposes the non-averaged potential is also plotted on the same figure). The 2D-cuts are function of the altitude of the projectile atom Z_p and the impact parameter b . These Boltzmann thermal averaged potentials have been generated by calculating the mean potential energy over a Boltzmann sampling of surface oscillator position for each position of the projectile in a plane where most of the ER recombination events are supposed to take place according to previous analysis⁴⁹ (see diagonal plane highlighted in Fig. 8). The potential bump at a projectile distance of about 2.5 \AA vanishes when going to the non-averaged potential to the temperature averaged ones. This effect is enforced when increasing the temperature. This observation is coherent with the slight decrease of the mean kinetic energy observed in Fig. 6 with temperature when projectiles experience the bump around 0.14 ps integration time. The attractive parts of the potential (depicted with bold dotted lines on Fig. 8) felt in average by the projectile atoms is slightly less attractive at 800 and 1500 K leading to the conclusion that the atoms should be less accelerated at higher temperature. As evaluated by the modified Baule model, a decrease of projectile kinetic energy before collision leads to a decrease of energy transfer. Less projectile energy transferred to the surface means more energy available for reactivity in a second step.

IV. CONCLUSIONS

QCT simulations have been performed to study the effect of a moving surface model (making use of the GLO scheme) to the energetics of the N_2 molecule formed via a direct ER mechanism. A FPLEPS model based on DFT calculations is used to integrate the equations of motion for our system. As already found for the $H + H/Ni(100)$ system,³² the significant amount of energy transferred into the surface inhibits reflection, and metastable hot atom formation increasing the cross section of atomic trapping and bound hot atom formation. The surface recoil also slightly lowers the direct ER reaction cross section. A simple one-collision Baule model for evaluating the mean energy transferred to the surface has shown its efficiency and provides simple arguments for understanding why the projectile energy transfer to the surface is lowered with an increase of the temperature. The analysis of the temperature averaged potential (Z_p , b)-2D cuts yields to the conclusion that the projectile acceleration is lowered upon surface mobility increase concomitant with temperature increase. Following the modified Baule model, the energy transfer is proportional to the projectile kinetic energy right before the collision. Thus, a projectile deceleration will cause a reduction of the energy released into the metal. Because most of the energy transferred to the surface is taken from the N_2 center of mass translational energy, the rotational and vibrational distributions are poorly affected by the surface motion. Such a result has already been noticed for the $H + H/Ni(100)$ system,

the main difference being the fact that $N + N/W(100)$ leads to highly excited molecules whereas not for $H + H/Ni(100)$.

- ¹K. Honkala, A. Hellman, I. Remediakis, A. Logadottir, A. Carlsson, S. Dahl, C. Christensen, and J. Norskov, *Science* **307**, 555 (2005).
- ²G. A. Somorjai, *Introduction to Surface Chemistry and Catalysis* (Wiley, New York, 1994).
- ³T. Rayment, R. Schlögl, J. M. Thomas, and G. Ertl, *Nature (London)* **315**, 311 (1985).
- ⁴M. J. Molina, L. T. Molina, and D. M. Golden, *J. Phys. Chem.* **100**, 12888 (1996).
- ⁵J. S. Mathis, *Rep. Prog. Phys.* **56**, 605 (1993).
- ⁶G. Winnewisser and E. Herbst, *Rep. Prog. Phys.* **56**, 1209 (1993).
- ⁷J. M. Greenberg, *Surf. Sci.* **500**, 793 (2002).
- ⁸A. W. Kleyn, N. J. L. Cardozo, and U. Samm, *Phys. Chem. Chem. Phys.* **8**, 1761 (2006).
- ⁹A. W. Kleyn, N. J. L. Cardozo, and W. Koppers, *Vacuum* **80**, 1098 (2006).
- ¹⁰V. Barabash, G. Federici, R. Matera, A. R. Raffray, and I. H. Teams, *Phys. Scr.* **T81**, 74 (1999).
- ¹¹G. Federici, C. H. Skinner, J. N. Brooks, J. P. Coad, C. Grisolia, A. A. Haasz *et al.*, *Nucl. Fusion* **41**, 1967 (2001).
- ¹²G. Federici, P. Andrew, P. Barabaschi, J. Brooks, R. Doerner, A. Geier, A. Herrmann, G. Janeschitz, K. Krieger, A. Kukushkin, A. Loarte, R. Neu, G. Saibene, M. Shimada, G. Strohmayer, and M. Sugihara, *J. Nucl. Mater.* **313-316**, 11 (2003).
- ¹³*Molecular Physics and Hypersonic Flows*, edited by M. Capitelli, NATO ASI Series C Vol. 482 (Kluwer Academic, Dordrecht, 1989).
- ¹⁴C. B. Duke and E. W. Plummer, *Frontiers in Surface and Interface Science* (Elsevier, Amsterdam, 2002).
- ¹⁵*Thin Films: Self-Assembled Monolayers of Thiols*, edited by A. Ulman, Vol. 24 (Academic Press Inc., San Diego, 1998).
- ¹⁶J. C. Love, L. A. Estroff, J. K. Kriebel, R. G. Nuzzo, and G. M. Whitesides, *Chem. Rev.* **105**, 1103 (2005).
- ¹⁷M. M. Biener, J. Biener, and C. M. Friend, *Langmuir* **21**, 1668 (2005).
- ¹⁸A. M. Wodtke, D. Matsiev, and D. J. Auerbach, *Prog. Surf. Sci.* **83**, 167 (2008).
- ¹⁹C. T. Rettner, D. J. Auerbach, J. C. Tully, and A. W. Kleyn, *J. Chem. Phys.* **100**, 13021 (1996).
- ²⁰G. J. Kroes, A. Gross, E. J. Baerends, M. Scheffler, and D. A. McCormack, *Acc. Chem. Res.* **35**, 193 (2002).
- ²¹*Theoretical Surface Science: A Microscopic Perspective*, edited by A. Gross, Advanced Texts in Physics (Springer, 2nd ed., 2009).
- ²²A. Gross, *Surf. Sci. Rep.* **32**, 291 (1998).
- ²³G. D. Billing, *Molecule Surface Interactions* (Wiley, New York, 2000).
- ²⁴G. R. Darling and S. Holloway, *Rep. Prog. Phys.* **58**, 1595 (1995).
- ²⁵C. T. Rettner, *Phys. Rev. Lett.* **69**, 383 (1992).
- ²⁶C. T. Rettner, *J. Chem. Phys.* **101**, 1529 (1994).
- ²⁷C. T. Rettner and D. J. Auerbach, *Phys. Rev. Lett.* **74**, 4551 (1995).
- ²⁸G. Lanzani, R. Martinazzo, G. Materzanini, I. Pino, and G. F. Tantardini, *Theor. Chem. Acc.* **117**, 805 (2007).
- ²⁹R. Martinazzo, S. Assoni, G. Marinoni, and G. F. Tantardini, *J. Chem. Phys.* **120**, 8761 (2004).
- ³⁰S. Caratzoulas, B. Jackson, and M. Persson, *J. Chem. Phys.* **107**, 6420 (1997).
- ³¹Z. B. Guvenc, X. Sha, and B. Jackson, *J. Chem. Phys.* **115**, 9018 (2001).
- ³²Z. B. Guvenc, X. Sha, and B. Jackson, *J. Phys. Chem. B* **106**, 8342 (2002).
- ³³B. Jackson and M. Persson, *J. Chem. Phys.* **96**, 2378 (1992).
- ³⁴B. Jackson and D. Lemoine, *J. Chem. Phys.* **114**, 474 (2001).
- ³⁵B. Jackson, X. Sha, and Z. B. Guvenc, *J. Chem. Phys.* **116**, 2599 (2002).
- ³⁶C. Kalyanaraman, D. Lemoine, and B. Jackson, *Phys. Chem. Chem. Phys.* **1**, 1351 (1999).
- ³⁷J. Kerwin and B. Jackson, *J. Chem. Phys.* **128**, 084702 (2008).
- ³⁸D. Lemoine, J. D. Quattrucci, and B. Jackson, *Phys. Rev. Lett.* **89**, 268302 (2002).
- ³⁹J. G. Quattrucci, B. Jackson, and D. Lemoine, *J. Chem. Phys.* **118**, 2357 (2003).
- ⁴⁰D. V. Shalashilin and B. Jackson, *J. Chem. Phys.* **109**, 2856 (1998).
- ⁴¹T. Kammler, D. Kolovos-Vellianitis, and J. Küppers, *Surf. Sci.* **460**, 91 (2000).
- ⁴²T. Kammler, S. Wehner, and J. Küppers, *J. Chem. Phys.* **109**, 4071 (1998).
- ⁴³D. V. Shalashilin, B. Jackson, and M. Persson, *J. Chem. Phys.* **110**, 11038 (1999).

- ⁴⁴D. V. Shalashilin, B. Jackson, and M. Persson, *Faraday Discuss.* **110**, 287 (1998).
- ⁴⁵J. Y. Kim and J. Lee, *J. Chem. Phys.* **113**, 2856 (2000).
- ⁴⁶J. Harris and B. Kasemo, *Surf. Sci.* **105**, L281 (1981).
- ⁴⁷L. Barrios, E. Quintas, L. Martin, C. Crespos, P. Larrégaray, J. Rubayo, and J.-C. Rayez, *Rev. Cub. Fis.* **28**, 61 (2011).
- ⁴⁸E. Quintas-Sánchez, L. Martin-Gondre, P. Larrégaray, C. Crespos, J. Rubayo-Soneira, and J.-C. Rayez, *Rev. Cub. Fis.* **27**, 244 (2010).
- ⁴⁹E. Quintas-Sánchez, P. Larrégaray, C. Crespos, L. Martin-Gondre, J. Rubayo-Soneira, and J.-C. Rayez, *J. Chem. Phys.* **137**, 064709 (2012).
- ⁵⁰M. Beult, K. D. Rendulic, and G. R. Castro, *Surf. Sci.* **385**, 97 (1997).
- ⁵¹C. T. Rettner, E. K. Schweizer, and H. Stein, *J. Chem. Phys.* **93**, 1442 (1990).
- ⁵²C. T. Rettner, H. Stein, and E. K. Schweizer, *J. Chem. Phys.* **89**, 3337 (1988).
- ⁵³C. T. Rettner, E. K. Schweizer, H. Stein, and D. J. Auerbach, *Phys. Rev. Lett.* **61**, 986 (1988).
- ⁵⁴H. E. Pfnür, C. T. Rettner, J. Lee, R. J. Madix, and D. J. Auerbach, *J. Chem. Phys.* **85**, 7452 (1986).
- ⁵⁵L. Martin-Gondre, C. Crespos, P. Larrégaray, J.-C. Rayez, B. van Ootegem, and D. Conte, *Chem. Phys. Lett.* **471**, 136 (2009).
- ⁵⁶L. Martin-Gondre, C. Crespos, P. Larrégaray, J.-C. Rayez, B. van Ootegem, and D. Conte, *J. Chem. Phys.* **132**, 204501 (2010).
- ⁵⁷L. Martin-Gondre, C. Crespos, P. Larrégaray, J.-C. Rayez, D. Conte, and B. van Ootegem, *Chem. Phys.* **367**, 136 (2010).
- ⁵⁸L. Martin-Gondre, M. Alducin, G. A. Bocan, R. Díez-Muiño, and J. I. Juaristi, *Phys. Rev. Lett.* **108**, 096101 (2012).
- ⁵⁹L. Martin-Gondre, G. A. Bocan, M. Alducin, J. I. Juaristi, and R. Díez-Muiño, *Comput. Theor. Chem.* **990**, 126–131 (2012).
- ⁶⁰M. Alducin, R. Díez-Muiño, H. F. Busnengo, and A. Salin, *J. Chem. Phys.* **125**, 144705 (2006).
- ⁶¹M. Alducin, R. Díez-Muiño, H. F. Busnengo, and A. Salin, *Phys. Lett.* **97**, 056102 (2006).
- ⁶²M. Alducin, R. Díez, H. F. Busnengo, and A. Salin, *Surf. Sci.* **601**, 3726 (2007).
- ⁶³G. Bocan, R. Díez, M. Alducin, and H. F. Busnengo, *J. Chem. Phys.* **128**, 154704 (2008).
- ⁶⁴G. Volpilhac, H. F. Busnengo, W. Dong, and A. Salin, *Surf. Sci.* **544**, 329 (2003).
- ⁶⁵G. Volpilhac and A. Salin, *Surf. Sci.* **556**, 129 (2004).
- ⁶⁶S. W. Singh-Boparail, M. Bowker, and D. A. King, *Surf. Sci.* **53**, 55 (1975).
- ⁶⁷P. W. Tamm and L. D. Smith, *Surf. Sci.* **26**, 286 (1971).
- ⁶⁸P. Hohenberg and W. Kohn, *Phys. Rev.* **136**, B864 (1964).
- ⁶⁹W. Kohn and L. J. Sham, *Phys. Rev.* **140**, A1133 (1965).
- ⁷⁰A. D. Becke, *Phys. Rev. A* **38**, 3098 (1988).
- ⁷¹J. P. Perdew, *Phys. Rev. B* **33**, 8822 (1986).
- ⁷²W. Dong and J. Hafner, *Phys. Rev. B* **56**, 15396 (1997).
- ⁷³A. Eichler, G. Kresse, and J. Hafner, *Phys. Rev. Lett.* **77**, 1119 (1996).
- ⁷⁴B. Hammer, M. Scheffler, K. W. Jacobsen, and J. K. Nørskov, *Phys. Rev. Lett.* **73**, 1400 (1994).
- ⁷⁵J. A. White, D. M. Bird, M. C. Payne, and I. Stich, *Phys. Rev. Lett.* **73**, 1404 (1994).
- ⁷⁶G. Wiesenekker, G. J. Kroes, E. J. Baerends, and R. C. Mowrey, *J. Chem. Phys.* **102**, 3873 (1995).
- ⁷⁷S. Wilke and M. Scheffler, *Surf. Sci. Lett.* **329**, L605 (1995).
- ⁷⁸H. F. Busnengo, W. Dong, P. Sautet, and A. Salin, *Phys. Rev. Lett.* **87**, 127601 (2001).
- ⁷⁹H. F. Busnengo, W. Dong, and A. Salin, *Phys. Rev. Lett.* **93**, 236103 (2004).
- ⁸⁰H. F. Busnengo, M. A. Di Césare, W. Dong, and A. Salin, *Phys. Rev. B* **72**, 125411 (2005).
- ⁸¹M. Dohle, P. Saalfrank, and T. Uzer, *J. Chem. Phys.* **108**, 4226 (1998).
- ⁸²S. A. Adelman, *J. Chem. Phys.* **71**, 4471 (1979).
- ⁸³J. C. Tully, *J. Chem. Phys.* **73**, 1975 (1980).
- ⁸⁴H.-J. Ernst, E. Hulpke, and J. P. Toennies, *Phys. Rev. B* **46**, 16081 (1992).
- ⁸⁵S. Titmuss, A. Wander, and D. A. King, *Chem. Rev.* **96**, 1291 (1996).
- ⁸⁶A. C. Luntz, I. Makkonen, M. Persson, S. Holloway, D. M. Bird, and M. S. Miziański, *Phys. Rev. Lett.* **102**, 109601 (2009).
- ⁸⁷J. I. Juaristi, M. Alducin, R. Díez-Muino, H. F. Busnengo, and A. Salin, *Phys. Rev. Lett.* **102**, 109602 (2009).
- ⁸⁸J. I. Juaristi, M. Alducin, R. Díez, H. F. Busnengo, and A. Salin, *Phys. Rev. Lett.* **100**, 116102 (2008).
- ⁸⁹I. Goikoetxea, J. I. Juaristi, M. Alducin, and R. Díez, *J. Phys: Condens. Matter* **21**, 264007 (2009).
- ⁹⁰G. J. Kroes, *Science* **321**, 794 (2008).
- ⁹¹C. T. Rettner, H. A. Michelsen, and D. J. Auerbach, *J. Chem. Phys.* **102**, 4625 (1995).
- ⁹²B. Baule, *Ann. Phys.* **349**, 145 (1914).
- ⁹³J. Harris, in *Dynamics of Gas-surface Interactions*, edited by C. T. Rettner and M. N. R. Ashfold (Royal Society of Chemistry, 1991).